THE JOURNAL OF BIOLOGICAL CHEMISTRY
Vol. 280, No. 9, Issue of March 4, pp. 8172–8179, 2005
Printed in U.S.A.

The 8-kDa Dynein Light Chain Binds to p53-binding Protein 1 and Mediates DNA Damage-induced p53 Nuclear Accumulation*

Received for publication, October 6, 2004, and in revised form, December 15, 2004
Published, JBC Papers in Press, December 20, 2004, DOI 10.1074/jbc.M411408200

Kevin W.-H. Lo‡§, Ho-Man Kan‡§, Ling-Nga Chan‡, Wei-Guang Xu‡, Ke-Peng Wang‡, Zhenguo Wu‡, Morgan Sheng¶‖, and Mingjie Zhang‡

From the ‡Department of Biochemistry, Hong Kong University of Science and Technology, Clear Water Bay, Kowloon, Hong Kong, People's Republic of China and ¶Picower Center for Learning and Memory, Howard Hughes Medical Institute, and Department of Brain and Cognitive Sciences, Massachusetts Institute of Technology, Cambridge, Massachusetts 02139

The tumor suppressor protein p53 is known to undergo cytoplasmic dynein-dependent nuclear translocation in response to DNA damage. However, the molecular link between p53 and the minus end-directed microtubule motor dynein complex has not been described. We report here that the 8-kDa light chain (LC8) of dynein binds to p53-binding protein 1 (53BP1). The LC8-binding domain was mapped to a short peptide segment immediately N-terminal to the kinetochore localization region of 53BP1. The LC8-binding domain is completely separated from the p53-binding domain in 53BP1. Therefore, 53BP1 can potentially act as an adaptor to assemble p53 to the dynein complex. Unlike other known LC8-binding proteins, 53BP1 contains two distinct LC8-binding motifs that are arranged in tandem. We further showed that 53BP1 can directly associate with the dynein complex. Disruption of the interaction between LC8 and 53BP1 *in vivo* prevented DNA damage-induced nuclear accumulation of p53. These data illustrate that LC8 is able to function as a versatile acceptor to link a wide spectrum of molecular cargoes to the dynein motor.

53BP1[1] is a large nuclear protein (1972 amino acid residues) that was originally identified as a p53-interacting protein in a yeast two-hybrid screen (1). The protein was subsequently characterized as an activator of p53-dependent gene transcription (2). The C-terminal end of 53BP1 contains two BRCA1 C terminus (BRCT) domains, a protein interaction module found in a number of proteins implicated in various aspects of cell cycle control, recombination, and DNA repair (3–7). The tandem BRCT repeats of 53BP1 are responsible for binding to p53 (Fig. 1, and Refs. 1, 8, 9). Upstream of the BRCT repeats resides a Tudor domain, a globular module shown to interact with dimethylated Arg (10). There are also multiple "(S/T)Q" motifs in the N-terminal region of 53BP1, and some of these (S/T)Q motifs have been shown to be phosphorylation sites of ataxia telangiectasia-mutated kinase (5, 11). It has been proposed that 53BP1 acts as an adaptor protein responsible for recruiting/assembling various proteins in the ataxia telangiectasia-mutated and ataxia telangiectasia-mutated and rad3-related signaling pathways (12).

In response to DNA damage, p53 accumulates in the nucleus (13–15), where it transcriptionally activates a number of genes (*e.g. p21* and *mdm2*) that are involved in growth arrest and apoptosis (16–19). The DNA damage-induced nuclear localization of p53 requires the minus end-directed microtubule motor dynein (20, 21). Disruption of the motor activity of dynein by microinjection of an antibody against the intermediate chain (IC74) of the motor or overexpressing dynamitin (p50) results in impaired accumulation of p53 in the nucleus following DNA damage (20). The molecular basis of dynein-mediated p53 nuclear trafficking is poorly understood, because p53 is not known to bind directly to the dynein motor complex. One would expect that certain adaptor protein(s) can act as a linker to couple p53 to the dynein motor. Identification of such adaptor protein(s) should provide insights into the dynein-mediated p53 nuclear trafficking. Recently, it was shown that hsp90/immunophilin complex might act as an adaptor to link p53 to a subunit of dynactin within the dynein motor complex in human colon cancer cells (22).

Cytoplasmic dynein is a multisubunit protein complex (~1.2 MDa) composed of two globular heads joined by flexible stalk domains to a common base. The base of the motor complex contains two 74-kDa intermediate chains (IC74), four light intermediate chains (52–61 kDa), and several light chains (10–25 kDa) (23, 24). The 8-kDa light chain (LC8, also named DLC8, PIN, and LC1) is a stoichiometric component of the cytoplasmic dynein complex (25). LC8 has been highly conserved throughout evolution and has been shown to bind to a large array of proteins with diverse cellular functions. For example, LC8 was found to bind specifically to neuronal nitric oxide synthase (26), to the proapoptotic member of the Bcl-2 family proteins Bim and Bmf (27, 28), to the product of the *Drosophila* swallow gene (29), to transcriptional regulator IκB (30), to guanylate kinase domain-associated protein (31), to viral phosphoproteins (32, 33), and to a number of proteins with unknown functions (34). It has been suggested that LC8 acts as a versatile adaptor that links cargo proteins to the dynein motor (34–37).

Here we report that LC8 specifically binds to 53BP1. Bio-

* This work was supported in part by the Research Grants Council of Hong Kong (Grants HKUST6207/00M, 6097/01M, and 6125/02M) and by a Philip Morris USA Inc. external research grant (to M. Z.). The costs of publication of this article were defrayed in part by the payment of page charges. This article must therefore be hereby marked "*advertisement*" in accordance with 18 U.S.C. Section 1734 solely to indicate this fact.

§ Both authors contributed equally to this work.
‖ An Investigator of the Howard Hughes Medical Institute.
** A Croucher Foundation Senior Research Fellow. To whom correspondence should be addressed. Tel.: 852-2358-8709; Fax: 852-2358-1552; E-mail: mzhang@ust.hk.

[1] The abbreviations used are: 53BP1, p53-binding protein 1; BRCT, BRCA1 C terminus domain; GFP, green fluorescent protein; GST, glutathione *S*-transferase; GSH, reduced glutathione; HEK, human embryonic kidney; IC74, dynein intermediate chain; LC8, 8-kDa dynein light chain; HA, hemagglutinin; PBS, phosphate-buffered saline; HIV-1, human immunodeficiency virus, type 1; ADR, adriamycin; nNOS, neuronal nitric-oxide synthase.

chemical dissection studies reveal that 53BP1 contains two distinct LC8-binding motifs that are arranged in tandem. Formation of the LC8·53BP1·p53 and 53BP1·LC8·dynein complexes suggests that 53BP1 can function to link p53 to the dynein complex. Disruption of the interaction between LC8 and 53BP1 *in vivo* prevented DNA damage-induced nuclear accumulation of p53. The data described in this work provide a distinct mechanism for dynein-mediated p53 nuclear trafficking.

MATERIALS AND METHODS

Yeast Two-hybrid Screening—Two-hybrid screening was performed as described previously (31). Briefly, LC8 was cloned into pBHA (LexA fusion vector) and used to screen $\sim 1 \times 10^6$ clones of a human cDNA library constructed in pGAD10 (GAL4 activation vector, Clontech).

Expression Constructs—The plasmid containing the full-length 53BP1 with an N-terminal hemagglutinin (HA) epitope and a histidine tag (pCMH6K53BP1) were provided by Dr. Kuniyoshi Iwabuchi. Truncation and deletion mutants of 53BP1 were generated by PCR cloning. The plasmid encoding GFP-fused p53 (GFP-p53) was provided by Dr. Randy Poon.

For bacterial expression of 53BP1 and its truncation mutants, the corresponding DNA fragments were individually cloned into the EcoRI/XhoI sites of the pGEX-4T1 expression vector (Amersham Biosciences). The GST-fused LC8 bacterial expression vector was generated by inserting LC8-coding DNA into the pGEX-4T1 vector by PCR cloning. The histidine-tagged p53 truncation mutant was constructed by inserting the p53 encoding gene into the EcoRI/BamHI sites of an in-house-modified pET32a vector.

Expression and Purification of Fusion Proteins—Bacterial expression of recombinant proteins was carried out using *Escherichia coli* BL21(DE3) as the host cells. To express GST-LC8 (or GST-53BP1), host cells containing the expression plasmid were grown in LB medium at 37 °C to an A_{600} of ~0.8. Expression of the fusion protein was induced by the addition of isopropyl-1-thio-β-D-galactopyranoside to a final concentration of ~0.25 mM. Protein expression continued for ~3 h at 37 °C before harvesting by centrifugation. The fusion proteins were expressed in soluble forms and purified using GSH-Sepharose affinity columns (Amersham Biosciences) following the manufacturer's instructions. The eluted proteins were dialyzed against phosphate-buffered saline (PBS) to remove the residual GSH. The dialyzed proteins were directly used for binding assay experiments. Expression of His_6-p53 proteins followed the procedure described for the expression of GST-LC8. His_6-p53 was purified by passing the cell lysate through a Ni^{2+}-nitrilotriacetic acid affinity column (Novagen). The N-terminal His tag of the fusion protein was cleaved by thrombin digestion. The cleaved His tag and other contaminating proteins were removed by passing the digestion mixture through a gel-filtration column. Preparation of purified, untagged LC8 has been described in our earlier work (38).

Cell Cultures and Transfection—HEK293 and H1299 cells were cultured in Dulbecco's modified essential medium containing 10% fetal bovine serum (Invitrogen) and penicillin/streptomycin at 37 °C in a humidified, 5% CO_2 incubator. For transient transfection, cells were plated on a 10-cm Petri dish (Falcon) to ~70% confluence and then were transfected with an appropriate amount of DNA using a Lipofectamine transfection kit (Invitrogen) following the manufacturer's instructions. Transient expression of transfected proteins was allowed to continue for 24–48 h.

Immunoblot Analysis—Anti-HA monoclonal antibody was purchased from Sigma, Anti-IC74 antibody was provided to us by Dr. K. Kevin Pfister, and anti-$p150^{Glued}$ antibody was from BD Biosciences. SDS-PAGE gel-resolved proteins were electrotransferred to a nitrocellulose membrane in a transferring buffer. Membranes were incubated with 10% skim milk, 0.1% Tween 20 in Tris-buffered saline and then probed with respective antibodies. Protein bands on Western blots were visualized by an enhanced chemiluminescent detection kit (ECL, Amersham Biosciences).

Pull-down Experiments—GST-LC8 (10 μg each) was mixed with HEK293 cell lysates (100 μg of total protein) containing HA-tagged full-length 53BP1 or HA-tagged 53BP1 truncation mutants. The GST-LC8-containing complexes were precipitated with fresh GSH-Sepharose beads. The pelleted beads were washed extensively with PBS buffer and subsequently boiled with 2× SDS-PAGE sample buffer. The proteins were first resolved by SDS-PAGE and subsequently analyzed by immunoblot analysis. The assay of the direct binding between LC8 and various purified GST fusion proteins followed the same method as described in our earlier work (34).

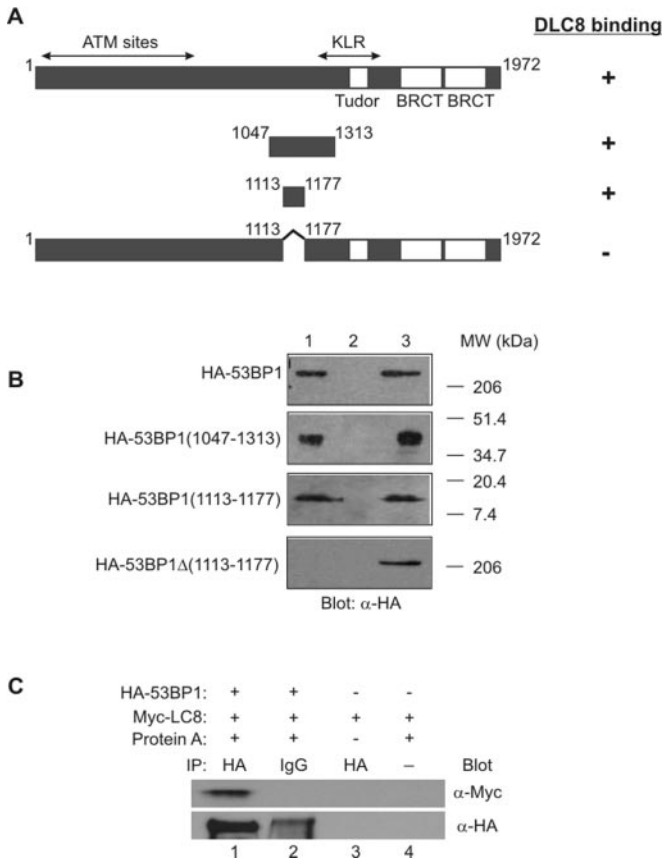

FIG. 1. **LC8 specifically binds to 53BP1.** *A*, schematic diagram showing the domain organization of 53BP1 and the truncation mutants of the protein used in the binding assay. The peptide fragment encoding residues 1047–1313 of 53BP1 was initially identified in the yeast two-hybrid screening. *B*, interaction between LC8 and various forms of 53BP1 *in vitro*. GST-LC8 was used to pull-down HA-tagged full-length 53BP1 (HA-53BP1) expressed in HEK293 cells (*lane 1*). Purified GST was used as the negative control (*lane 2*). *Lane 3* shows 10% of 53BP1 input used in the pull-down assays. Molecular mass markers are indicated on the *left*. *C*, *in vivo* association of LC8 and 53BP1. When co-expressed in HEK293 cells, HA-53BP1 and Myc-tagged LC8 could be co-immunoprecipitated with anti-HA antibody (*lane 1*). *Lanes 2–4* serve as various controls for the binding experiment.

HIV-1 Tat Fusion Peptide Experiments—The following peptides were synthesized and HPLC-purified. The underlined sequences of the peptides correspond to the protein transduction domain of HIV-1 Tat amino acid 47–57 (Tat). YGRKKRRQRRRSYSKSTQTT (Tat-KSTQTT) and YGRKKRRQRRRSYSKSAAAT (Tat-KSAAAT). H1299 cells transfected with GFP-p53 were washed with PBS and replenished with fresh Dulbecco's modified essential medium. Adriamycin (ADR, 0.4 μg/ml) and different concentrations of Tat-peptides were added into the medium and incubated at 37 °C for 60 min. Fresh fetal bovine serum was added to the cells to a final concentration of 10%, and cells were cultured for another 2 h. At this point, the cells were washed twice with PBS, fixed with 4% paraformaldehyde/PBS, and permeabilized with 0.2% Triton X-100/PBS. The nuclei were stained with 4′,6-diamidino-2-phenylindole and then examined by fluorescence microscopy.

RESULTS

Identification of 53BP1 as a LC8-binding Protein—A yeast two-hybrid screen of a human brain cDNA library using LC8 as the bait was carried out to identify potential LC8-binding proteins. Among many positive clones identified (34), one encodes a fragment of 53BP1 (residues 1047–1313, Fig. 1*A*). The interaction between LC8 and 53BP1 was confirmed in an *in vitro* pull-down experiment (Fig. 1*B*). When expressed in HEK293 cells, the 53BP1 fragment isolated from the yeast two-hybrid screen was shown to interact robustly with GST-LC8 (Fig. 1*B*, *lane 1* in the *second panel*). In addition, HA-tagged, full-length

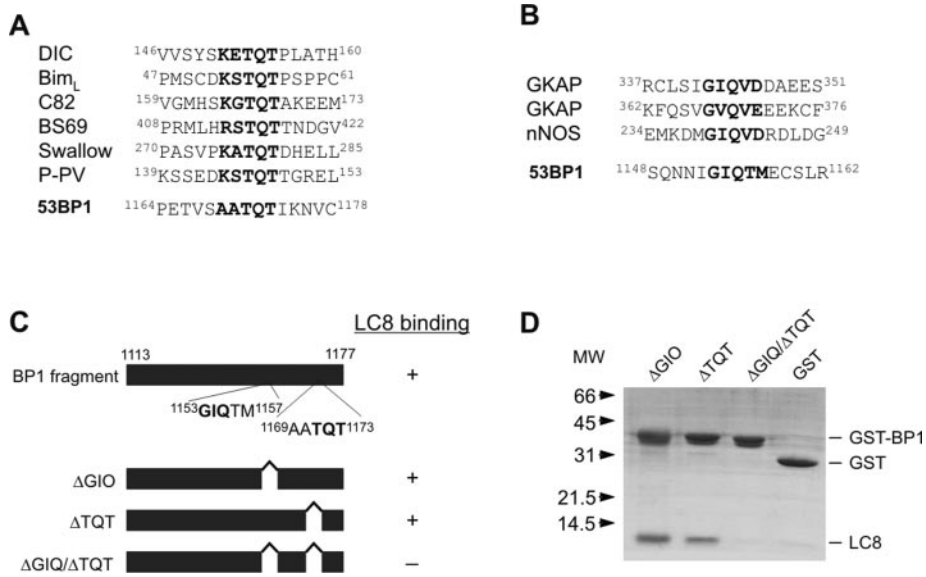

FIG. 2. **53BP1 contains two distinct LC8-binding motifs.** *A*, amino acid sequence alignment of LC8-binding domains from selected target proteins containing the consensus (K/R)*X*TQT motif. The (K/R)*X*TQT-like sequence of 53BP1 is shown at the *bottom*. *B*, sequence alignment of GIQVD motifs of selected LC8-binding proteins. The GIQVD-like motif of 53BP1 is indicated at the *bottom* of the *panel*. *C*, schematic diagram showing the GST-53BP1 deletion mutants used to map the LC8 binding sequences of the protein. The amino acid sequences of the two potential LC8-interacting motifs are included in the figure. *D*, Coomassie Blue staining of SDS-PAGE gel showing the interactions between various GST-53BP1 deletion mutants and LC8. The lane labeled "*GST*" serves as a negative control.

53BP1 could be specifically and robustly pelleted by purified recombinant GST-LC8 attached to GSH-Sepharose beads (Fig. 1*B*, *lane 1* in the *first panel*). When the two proteins were co-expressed in HEK293 cells, 53BP1 and LC8 formed a tight complex that could be efficiently immunoprecipitated from cell lysates (Fig. 1*C*, *lane 1*).

The LC8-binding fragment of 53BP1 isolated from the yeast two-hybrid screen partially overlapped with the KLR domain of the protein. Removal of the amino acid residues that overlap with the KLR domain (residues 1178–1313) generated a 65-residue peptide fragment corresponding to amino acid residues 1113–1177 of 53BP1. This 65-residue fragment was found to bind robustly to LC8 (Fig. 1*B*, *lane 1* in the *third panel*). Deletion of this 65-residue fragment from the full-length 53BP1 completely abolished its binding to LC8 (Fig. 1*B*, *lane 1* in the *bottom panel*). Taken together, the data in Fig. 1 demonstrate that 53BP1 can specifically bind to LC8, and the 65-residue fragment N-terminal to the KLR domain is necessary and sufficient for 53BP1 to bind to LC8.

53BP1 Contains Two Distinct LC8-binding Motifs—In our earlier work, we showed that LC8 binds to multiple target proteins via a consensus (R/K)*X*TQT motif (where "*X*" is variable amino acids) (Fig. 2*A* and Ref. 34). Inspection of the amino acid sequence reveals that the ^{1169}AATQT^{1173} sequence within the 65-residue LC8-binding fragment of 53BP1 resembles this consensus LC8-binding motif (Fig. 2*C*). To determine whether the ^{1169}AATQT^{1173} sequence is indeed the LC8-binding motif of 53BP1, we deleted three residues (TQT) from the 65-residue LC8-binding fragment of 53BP1 (Fig. 2*C*). Earlier biochemical and structural studies indicated that deletion of the TQT cassette from the consensus (R/K)*X*TQT motif was sufficient to disrupt its LC8-binding capacity (34, 36). To our surprise, the $^{1171\Delta}$TQT^{1173} deletion mutant of 53BP1 could still bind to LC8 (Fig. 2*D*, *second lane*). This outcome suggested that either the ^{1169}AATQT^{1173} sequence is not the authentic LC8-binding motif or this sequence is not the only LC8-binding motif. It is known that some LC8 target proteins do not contain the (R/K)*X*TQT motif in their LC8-binding domains (31, 34, 36, 39, 40). For example, the ^{239}GIQVD^{243} sequence of neuronal nitric-oxide synthase (nNOS) plays a central role in the binding of the enzyme to LC8 (36, 39). We also found that another LC8-binding protein, GKAP, contains two GIQVD-like motifs (Fig. 2*B*) and that both motifs are involved in LC8-binding.[2] The 65-residue LC8-binding fragment of 53BP1 also contains a GIQVD-like motif (^{1153}GIQTM^{1157}). This motif is located slightly upstream of the ^{1169}AATQT^{1173} motif (Fig. 2, *B* and *C*). To test if the ^{1153}GIQTM^{1157} motif of 53BP1 plays an active role in LC8 binding, we deleted the ^{1153}GIQ^{1155} cassette from the 65-residue LC8-binding segment of 53BP1 and assayed the LC8-binding capacity of the mutant. Again, based on earlier structural and mutagenesis studies, deletion of the GIQ-cassette would abrogate the GIQVD motif-mediated LC8 binding (36, 39). In contrast to our prediction, the ^{1153}GIQ^{1155}-deletion mutant of 53BP1 also interacted with LC8 (Fig. 2*D*, *first lane*), indicating the involvement of other regions of 53BP1 in LC8 binding. We next generated a double deletion mutant with both the ^{1153}GIQ^{1155} and the ^{1171}TQT^{1173} cassettes removed. This double mutant showed no detectable LC8 binding (Fig. 2*D*, *third lane*). Taken together, we conclude that 53BP1 contains two distinct LC8-binding motifs with amino acid sequences of ^{1153}GIQTM^{1157} and ^{1169}AATQT^{1173}.

We expect that the ^{1169}AATQT^{1173} motif of 53BP1 binds to LC8 in an essentially identical manner as does the (R/K)*X*TQT motif, because we earlier showed that mutation of the positively charged Arg/Lys in the motif to an Ala introduced very limited changes to LC8 binding (34). Therefore, we chose not to characterize the interaction between the ^{1169}AATQT^{1173} motif of 53BP1 and LC8 in further detail. In contrast, the nature of the interaction between the ^{1153}GIQTM^{1157} motif of 53BP1 and LC8 remains uncertain because of the sequence divergence between this motif and the LC8-binding domain of nNOS (the only well characterized LC8-binding protein without an (R/K)*X*TQT motif). We next studied the interaction between the ^{1153}GIQTM^{1157} motif of 53BP1 and LC8 in more detail. To test the binding of the GIQTM motif to LC8, we used a 13-residue synthetic peptide corresponding to ^{1149}QNNI**GIQTM**ECSL^{1161} of 53BP1 (called the GIQ-peptide here), and titrated ^{15}N-la-

[2] K. W.-H. Lo, H.-M. Kan, and M. Zhang, our unpublished data.

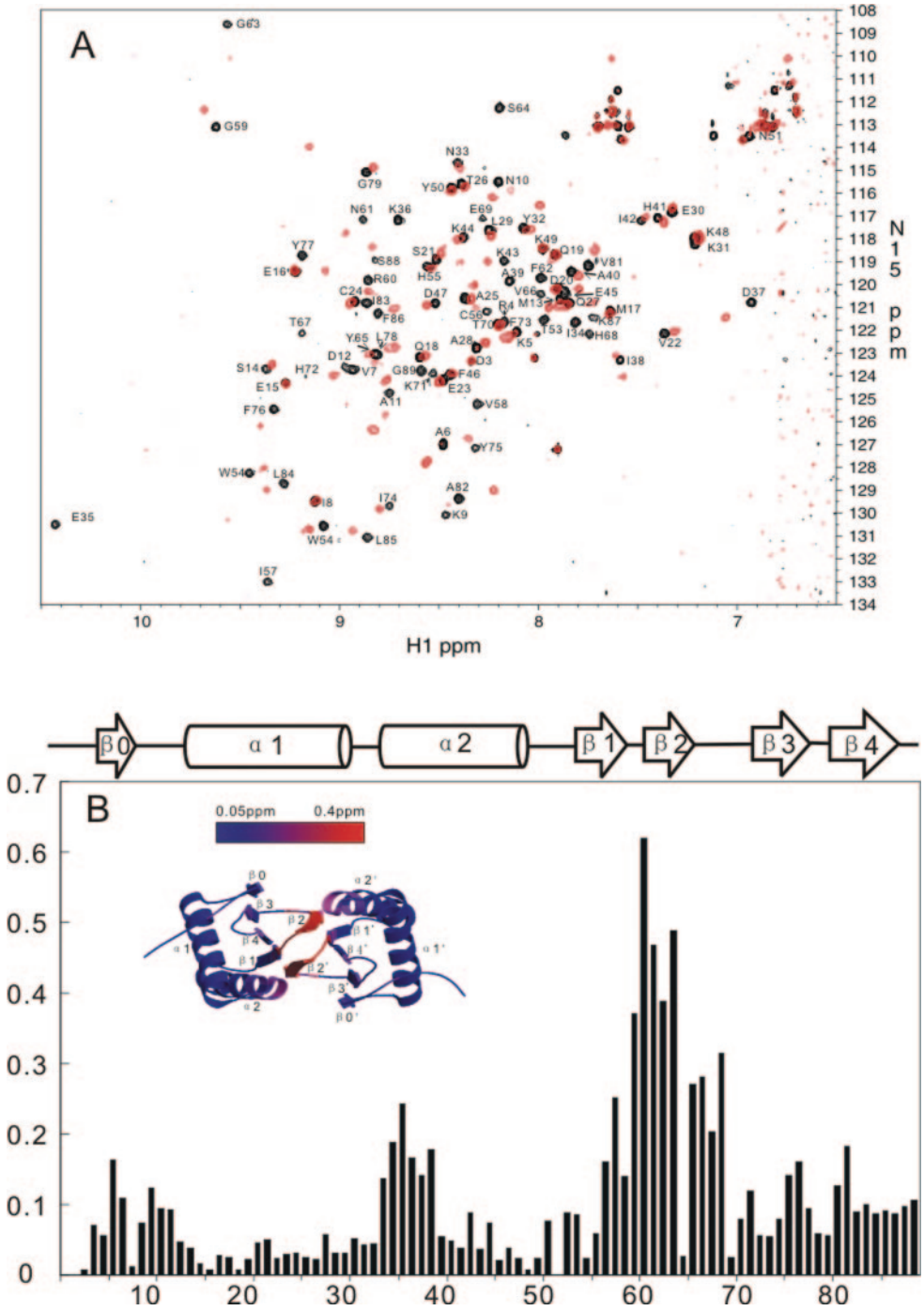

FIG. 3. **The GIQ-peptide of 53BP1 binds to LC8 with high affinity.** *A*, superposition plot of the ^{1}H,^{15}N HSQC spectra of free (*black*) and the GIQ-peptide saturated (*red*) LC8. The assignment of the free form LC8 is labeled with each amino acid residue name and number. *B*, plot as a function of the residue number of combined ^{1}H and ^{15}N chemical shift changes of LC8 induced by the GIQ-peptide binding. The combined ^{1}H and ^{15}N chemical shift changes are defined as: $\Delta_{ppm} = [(\Delta\delta_{HN})^2 + (\Delta\delta_N \times \alpha_N)^2]^{1/2}$, where $\Delta\delta_{HN}$ and $\Delta\delta_N$ represent chemical shift differences of amide proton and nitrogen chemical shifts of free LC8 and the protein in complex with the GIQ-peptide, respectively. The scaling factor (α_N) used to normalize the ^{1}H and ^{15}N chemical shifts is 0.17. The secondary structure of LC8 is indicated at the *top of the plot*. The *inset* shows the amplitude (in *pseudo-color scale*) of the GIQ-peptide-induced chemical shift changes of LC8 mapped on to the three-dimensional structure of the LC8 dimer.

beled LC8 with the peptide using NMR spectroscopy. In the presence of sub-stoichiometric amount of the GIQ-peptide, we observed two distinct sets of backbone amide peaks in the ^{1}H,^{15}N HSQC spectra of LC8/peptide mixtures. These two sets of resonances correspond to the peptide-bound form and the free form of LC8. The slow exchange of the peptide-bound form and the free form of LC8 observed in the NMR sample tube indicate that the GIQ-peptide binds to LC8 with high affinity. The LC8 dimer was saturated upon addition of a two molar ratio of the GIQ-peptide (Fig. 3*A*), indicating that each LC8 dimer binds to two molecules of the GIQ-peptide. The specificity of the binding of the GIQ-peptide to LC8 was further demonstrated by the does-dependent competition between the GIQ-peptide and the full-length 53BP1 for binding to LC8 (Fig. 4*A*).

We next investigated which regions of LC8 are involved in the GIQ-peptide binding. We used the well established minimum chemical shift perturbation approach to map the GIQ-peptide-binding region on LC8 by taking the advantage of complete chemical shift assignment of the free form of LC8 (36). Fig. 3*B* summarizes the chemical shift changes of LC8 induced

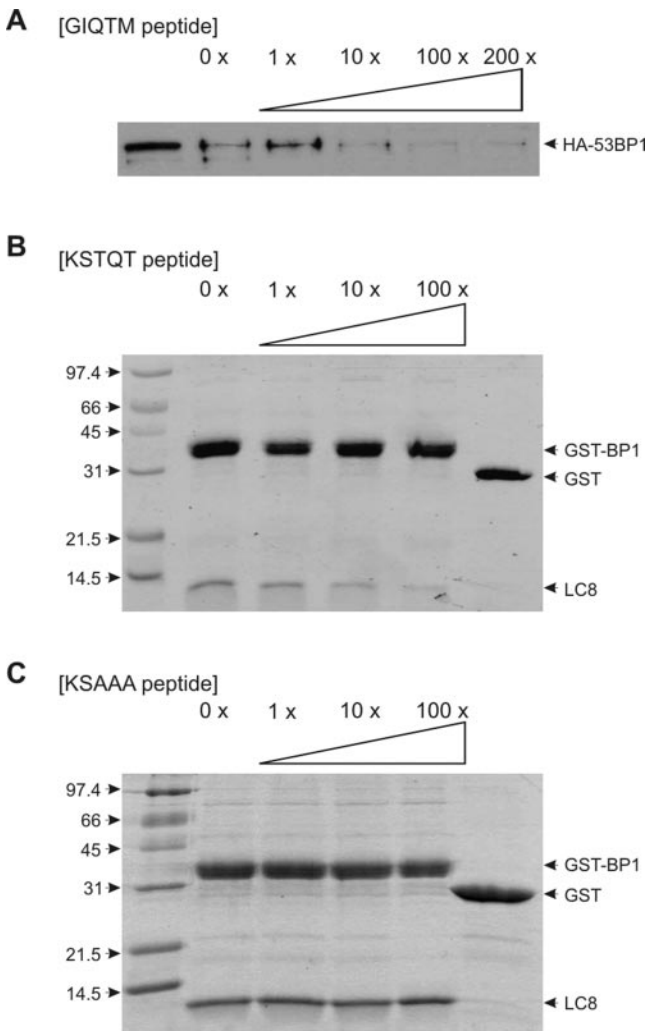

FIG. 4. **Synthetic peptides containing either class of LC8-binding motifs specifically compete with 53BP1 for binding to LC8.** *A*, the GIQ-peptide competes with 53BP1 for LC8 in a dose-dependent manner. Due to the limited solubility of the GIQ-peptide in the aqueous buffer, a peptide stock solution was prepared by dissolving the sample in Me_2SO. The volume of Me_2SO was kept to <5% of the total volume and remained the same in each assay mixture. *B*, the KSTQT-peptide competes for binding to with 53BP1 for LC8 in a similar dose-dependent manner as the GIQ-peptide. *C*, substitution of the critical TQT cassette with the AAA cassette in the KSTQT-peptide completely abolished the LC8-binding capacity of the peptide.

by the GIQ-peptide binding. The *inset* in Fig. 3*B* shows the GIQ-peptide-induced chemical shift changes mapped on to the backbone structure of the LC8 dimer (36). The data clearly show that amino acid residues in the β2-strand, β1/β2-loop, β2/β3-loop, and the N-terminal part of α2-helix are involved in the GIQ-peptide binding. The GIQ motif peptide-induced chemical shift perturbation profile of LC8 is highly similar to that induced by the LC8-binding peptide derived from nNOS (36, 38). Therefore, we conclude that the GIQ-peptide of 53BP1 is likely to bind to the common target accommodating groove of LC8 by forming antiparallel β-sheet with the β2-strand of LC8 (36). Furthermore, the GIQ motif represents another consensus LC8-binding sequence found in a number of LC8 target proteins, including 53BP1, nNOS, and GKAP (Fig. 2*B*).

53BP1 Forms a Ternary Complex with LC8 and p53—Because the LC8-binding domain and the p53-binding domain on 53BP1 do not overlap, we hypothesized that 53BP1 may function as a scaffold protein assembling p53 and LC8 into a protein complex. To test this hypothesis, we assayed the potential ternary complex formation using purified recombinant GST-53BP1, p53, and LC8. We used the DNA-binding core domain (residues 94–292) of p53 for the binding assay as this fragment is known to be sufficient for binding to 53BP1 (8, 9). Data in Fig. 5*A* demonstrate that GST-53BP1 can simultaneously bind to p53 and LC8 (*lane 1*). As expected, GST-53BP1 can efficiently bind to p53 only when these two proteins are mixed (Fig. 5*A*, *lane 2*, and Fig. 5*B*, *lane 2 top panel*). In contrast, no direct interaction was observed between p53 and LC8 (Fig. 5*B*, *lane 2 bottom panel*). Consistent with the observation shown in Fig. 5*A*, GST-LC8 can pull-down p53 only when 53BP1 is co-expressed in HEK293 cells (Fig. 5*C*, *lane 2*).

We then asked whether 53BP1 can directly associate with the dynein complex. This is particularly relevant for establishing a physical connection between the LC8·53BP1 complex and the dynein motor, because LC8 has been found to bind to a number of proteins other than the dynein complex. We overexpressed HA-53BP1 in HEK293 cells and found that HA-53BP1 could specifically pull down the endogenous intermediate chain as well as the $p150^{Glued}$ dynactin subunit of the cytoplasmic dynein complex (Fig. 5*D*). Taken together, the data shown in Fig. 5 indicated that LC8 is capable of linking the 53BP1 to the dynein complex *in vivo*.

The LC8/53BP1 Interaction Regulates DNA Damage-induced p53 Nuclear Accumulation—Recently, it has been demonstrated that the functional dynein is required for DNA damage-induced p53 nuclear accumulation (20, 21). However, the molecular mechanism of the dynein-dependent nuclear accumulation of p53 has not been described. The formation of the p53·53BP1·LC8 complex described in this work suggests that LC8 may link the p53·53BP1 complex to the dynein motor. If this prediction were true, disruption of the LC8·53BP1 interaction would compromise dynein-dependent p53 nuclear accumulation. To disrupt the interaction between LC8 and 53BP1, we used a 9-residue synthetic peptide with amino acid sequence of SYSKSTQTT (referred to as KSTQT-peptide). This peptide contains the well characterized K*X*TQT motif and specifically binds to the target-receiving grooves of the LC8 dimer (34, 36, 37). As expected, this KSTQT peptide was able to disrupt the LC8·53BP1 interaction in a does-dependent manner (Fig. 4*B*). A control peptide with Ala residues replacing both the Thr and Glu residues in the K*X*TQT motif (called the KSAAA-peptide) was not able to disrupt the LC8–53BP1 interaction (Fig. 4*C*). To test the function of the LC8·53BP1 complex in p53 nuclear accumulation *in vivo*, we fused the KSTQT motif peptide to the C terminus of the membrane penetrating domain of HIV-1 Tat (Tat-KSTQT peptide) (41, 42). Tat-fused peptides are widely used to facilitate internalization of synthetic peptides into living cells (41, 43). Inclusion of micromolar concentration of the Tat-KSTQT peptide in the cell culture media resulted in significant reduction of ADR-mediated p53 nuclear accumulation (Fig. 6*A*, *left panels*). Quantitative analysis showed that the Tat-KSTQT-mediated block of p53 nuclear accumulation is dose-dependent (Fig. 6*B*). At a peptide concentration of ~50 μM in the culture media, p53 remained in the cytoplasm in the majority of the cells (Fig. 6, *A* and *B*). Consistent with earlier studies, nearly all cells showed exclusive nuclear localization of p53 when the Tat-KSTQT peptide was left out of the culture medium (Fig. 6*B* and Refs. 20 and 21). In contrast, inclusion of the Tat-KSAAA-peptide in the culture medium at concentrations up to 50 μM did not lead to detectable inhibition of ADR-mediated p53 nuclear accumulation (Fig. 6*A*, *central panels*). As a control, p53 displayed diffused localizations in both cytoplasm and nucleus when neither the Tat-KSTQT peptide nor ADR was included in the culture media (Fig. 6*A*, *right panels*). To eliminate potential artifacts that might be introduced by the Tat fusion tag, we used the C

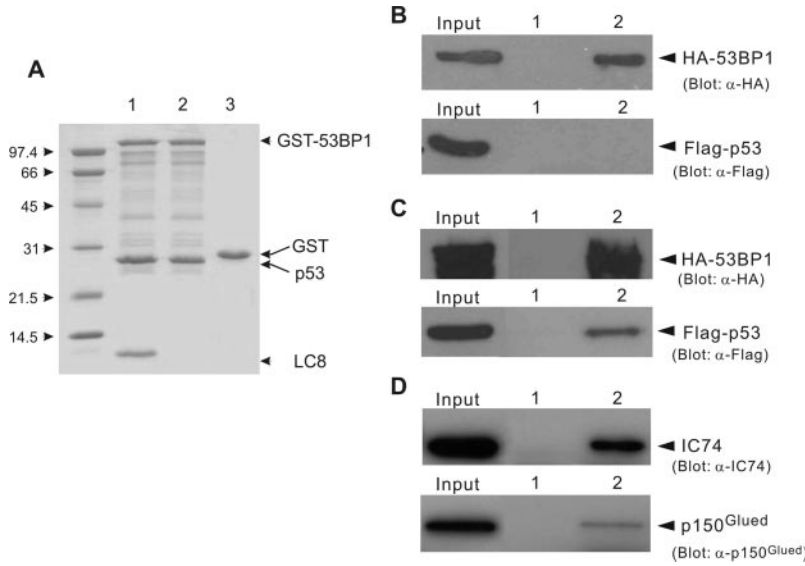

FIG. 5. **Dynein, LC8, 53BP1, and p53 can associate with each other.** *A*, Coomassie Blue staining of the SDS-PAGE gel showing that the GST-53BP1 fragment can simultaneously interact with LC8 and p53 (*lane 1*). *Lane 2* shows that GST-BP1 can directly interact with p53. *Lane 3* serves as a negative control showing that GST does not interact with p53 or LC8. *B*, pull-down analysis showing that GST-LC8 efficiently binds to HA-tagged 53BP1 overexpressed in HEK293 cells (*lane 2*, *top panel*). In contrast, GST-LC8 did not bind to p53 overexpressed in the same cell line (*lane 2*, *bottom panel*). *C*, pull-down assay showing that when p53 and 53BP1 were co-expressed in HEK293 cells, GST-LC8 can pull-down 53BP1 (*lane 2*, *top panel*) as well as p53 (*lane 2*, *bottom panel*). *Lane 1* in both panels *B* and *C* serve to show that GST does not bind to 53BP1 or to p53. *D*, direct association of 53BP1 with the dynein complex. HA-tagged 53BP1 was overexpressed in HEK293 cells. Immunoprecipitation of 53BP1 with anti-HA antibody co-precipitated both the intermediate chain (*lane 2*, *top panel*) and the $p150^{Glued}$ dynactin subunit (*lane 2*, *bottom panel*) of the cytoplasmic dynein complex. *Lane 1* in both panels shows that HEK293 cells transfected with an empty vector containing the HA-tag pulled down neither IC74 nor $p150^{Glued}$.

terminus of the Antennapedia homeodomain peptide (Antp) to facilitate internalization of synthetic peptides into living cells (41, 43). We observed that the Antp-KSTQT peptide displayed a similar dose-dependent inhibition of ADR-mediated GFP-p53 nuclear accumulation (data not shown).

DISCUSSION

In this work, we discovered that 53BP1 is a specific binding partner of LC8, the smallest light chain of cytoplasmic dynein. We further showed that 53BP1 can act as an adaptor to assemble p53 and LC8 into a ternary complex. Additionally, we demonstrated that 53BP1 can directly associate with the dynein complex. We note that 53BP1 is a unique LC8-binding partner when compared with numerous known LC8-binding proteins. 53BP1 contains two distinct LC8-binding motifs located ~10 residues apart (^{1153}GIQTM^{1157} and ^{1169}AATQT^{1173}). The LC8 binding motifs are located upstream of the KLR domain and do not overlap with any known protein binding sites on 53BP1. Of the two LC8-binding motifs, one (the ^{1169}AATQT^{1173} motif) is highly similar to the previously identified (K/R)*X*TQT motif (34). In our earlier study, we showed that mutation of the positively charged Lys to an Ala in the (K/R)*X*TQT motif had a very limited impact on the binding of the peptide to LC8. Therefore, the synthetic peptide containing the ^{1169}AATQT^{1173} motif of 53BP1 is likely to be a fully functional LC8-binding peptide. The other specific LC8-binding motif (the ^{1153}GIQTM^{1157} motif) resembles the GIQVD LC8-binding sequence identified in nNOS (36, 38, 39) and GKAP (40). We conclude that the GIQVD-like motif represents another consensus LC8-binding sequence in addition to the previously identified (K/R)*X*TQT motif. Identification of the second general LC8-binding motif will help us to understand the interactions between LC8 and a growing number of target proteins.

It is somewhat intriguing that 53BP1 contains two distinct LC8-binding motifs in 53BP1. Biochemical and structural studies have shown that both motifs, when isolated, are able to bind specifically to LC8 (Refs. 36 and 39 and this study). The LC8 dimer is likely to be assembled into the dynein motor by binding to the KETQT motif of the dynein intermediate chain using one of its two symmetric binding grooves (34, 44). It has been proposed that the other target binding groove of the LC8 dimer is used to attach cargo proteins to be transported to the dynein complex (36). Under this scenario, one LC8-binding motif should be sufficient for 53BP1 to attach to the dynein motor. It is possible that one of the LC8-binding motifs identified from this study is accessible in the full-length 53BP1 under cellular conditions. The other possible explanation for having two LC8-binding sites immediately next to each other within one protein is to raise the LC8 target concentration, such that 53BP1 is always attached to the dynein complex. Our *in vitro* binding studies indeed showed that the full-length 53BP1 and its fragments containing both LC8-binding sites all showed stronger binding to LC8. However, we were not able to obtain quantitative binding data between 53BP1 and LC8 due to the poor quality of the recombinant 53BP1.

The identification of 53BP1 as a binding partner of the dynein complex suggests that 53BP1 can function as an adaptor protein capable of linking p53 as well as other 53BP1-binding proteins to the microtubule motor. Our finding provides a possible molecular explanation for dynein-mediated p53 nuclear accumulation (20, 21). Consistent with this notion, disruption of the interaction between 53BP1 and LC8 (and therefore the dynein complex) *in vivo* using a cell-permeable LC8-binding inhibitory peptide (Tat-KSTQT-peptide) compromised DNA damage-induced p53 nuclear accumulation (Fig. 6). Although less likely, it is possible that the Tat-KSTQT-peptide-induced p53 trafficking changes might result from changes of interactions between LC8 and its binding targets other than the dynein complex, considering that the majority of cellular LC8 is not associated with dynein (25). Recently, it was reported that the hsp90·immunophilin complex can also function as an adaptor to linker p53 to the dynein motor in human colon cancer

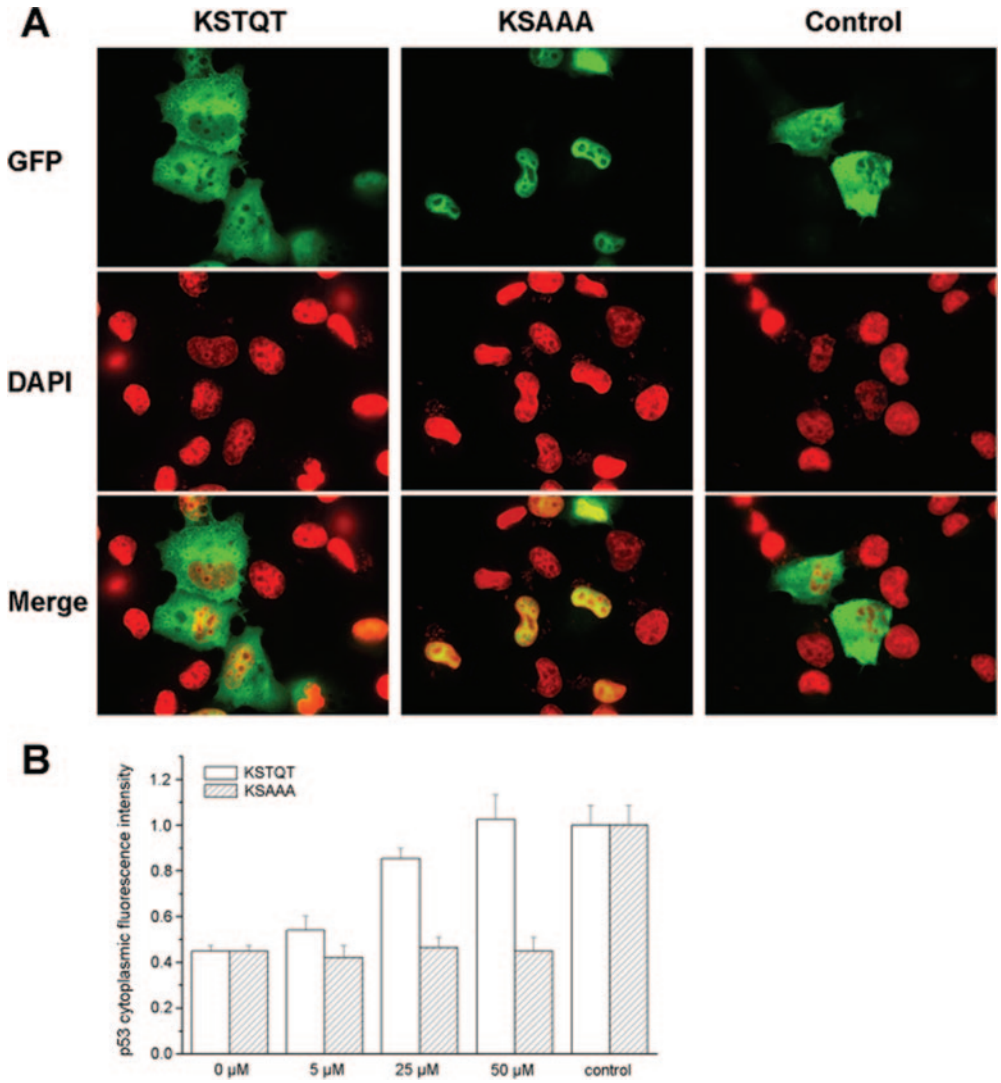

FIG. 6. **Disruption of the LC8/53BP1 interaction prevents ADR-mediated p53 nuclear accumulation.** *A*, representative fields of fluorescence microscopic images showing the distribution of GFP-p53 in the presence of 50 μM Tat-KSTQT peptide in the cell culture medium (*left panels*). The images in the *central panels* show the distribution of GFP-p53 in the presence of 50 μM Tat-KSAAA peptide. The images at the *right panels* show GFP-p53 distribution without addition of ADR in the culture medium. 4′,6-Diamidino-2-phenylindole staining marks the nuclei of the cells. *B*, quantification of the dose-dependent inhibition of GFP-p53 nuclear accumulation by the Tat-KSTQT peptide. The integrated value of cytoplasmic GFP-p53 fluorescence intensity at each peptide concentration was used for quantification. The fluorescence intensities at various peptide concentrations were normalized to the GFP-p53 intensity of the control culture (without addition of ADR and Tat-KSTQT peptide). The results shown are the averages of three independent experiments.

cells (22). Given the paramount functions of p53, it is perhaps not surprising that multiple molecular mechanisms are involved in transporting p53 to nuclei in response to different stress signals.

53BP1 is a large multimodular protein containing ~2000 amino acid residues. The protein functions as an adaptor/scaffold capable of binding to a large array of proteins in the ataxia telangiectasia-mutated and ataxia telangiectasia-mutated and rad3-related signaling pathways (12). One can envisage that the protein complexes assembled by 53BP1 are extremely large and that such complexes will need molecular motors such as dynein to be actively transported in living cells. Under most cellular conditions, 53BP1 is localized in the nucleus (3–5, 45). It is possible that the dynein complex plays an active role in constitutively shuttling 53BP1 complexes into the cell nuclei. Further experiments are required to test this hypothesis.

Acknowledgments—We thank Drs. Kuniyoshi Iwabuchi and Randy Poon for providing us with the cDNAs encoding 53BP1 and GFP-p53, respectively; Dr. K. Kevin Pfister for the IC74 antibody.

REFERENCES

1. Iwabuchi, K., Bartel, P. L., Li, B., Marraccino, R., and Fields, S. (1994) *Proc. Natl. Acad. Sci. U. S. A.* **91,** 6098–6102
2. Iwabuchi, K., Li, B., Massa, H. F., Trask, B. J., Date, T., and Fields, S. (1998) *J. Biol. Chem.* **273,** 26061–26068
3. Rappold, I., Iwabuchi, K., Date, T., and Chen, J. (2001) *J. Cell Biol.* **153,** 613–620
4. Schultz, L. B., Chehab, N. H., Malikzay, A., and Halazonetis, T. D. (2000) *J. Cell Biol.* **151,** 1381–1390
5. Anderson, L., Henderson, C., and Adachi, Y. (2001) *Mol. Cell. Biol.* **21,** 1719–1729
6. Manke, I. A., Lowery, D. M., Nguyen, A., and Yaffe, M. B. (2003) *Science* **302,** 636–639
7. Yu, X., Chini, C. C. S., He, M., Mer, G., and Chen, J. (2003) *Science* **302,** 639–642
8. Joo, W. S., Jeffrey, P. D., Cantor, S. B., Finnin, M. S., Livingston, D. M., and Pavletich, N. P. (2002) *Genes Dev.* **16,** 583–593
9. Derbyshire, D. J., Basu, B. P., Serpell, L. C., Joo, W. S., Date, T., Iwabuchi, K., and Doherty, A. J. (2002) *EMBO J.* **21,** 3863–3872
10. Maurer-Stroh, S., Dickens, N. J., Hughes-Davies, L., Kouzarides, T., Eisenhaber, F., and Ponting, C. P. (2003) *Trends Biochem. Sci.* **28,** 69–74
11. DiTullio, R. A., Jr., Mochan, T. A., Venere, M., Bartkova, J., Sehested, M., Bartek, J., and Halazonetis, T. D. (2002) *Nat. Cell Biol.* **4,** 998–1002
12. Wang, B., Matsuoka, S., Carpenter, P. B., and Elledge, S. J. (2002) *Science* **298,** 1435–1438
13. Kastan, M. B., Onyekwere, O., Sidransky, D., Vogelstein, B., and Craig, R. W.

(1991) *Cancer Res.* **51,** 6304–6311
14. Lane, D. P. (1992) *Nature* **358,** 15–16
15. Prives, C. (1998) *Cell* **95,** 5–8
16. Callebaut, I., and Mornon, J. P. (1997) *FEBS Lett.* **400,** 25–30
17. Levine, A. J. (1997) *Cell* **88,** 323–331
18. el-Deiry, W. S., Tokino, T., Velculescu, V. E., Levy, D. B., Parsons, R., Trent, J. M., Lin, D., Mercer, W. E., Kinzler, K. W., and Vogelstein, B. (1993) *Cell* **75,** 817–825
19. Miyashita, T., and Reed, J. C. (1995) *Cell* **80,** 293–299
20. Giannakakou, P., Sackett, D. L., Ward, Y., Webster, K. R., Blagosklonny, M. V., and Fojo, T. (2000) *Nat. Cell Biol.* **2,** 709–717
21. Giannakakou, P., Nakano, M., Nicolaou, K. C., O'Brate, A., Yu, J., Blagosklonny, M. V., Greber, U. F., and Fojo, T. (2002) *Proc. Natl. Acad. Sci. U. S. A.* **99,** 10855–10860
22. Galigniana, M. D., Harrell, J. M., O'Hagen, H. M., Ljungman, M., and Pratt, W. B. (2004) *J. Biol. Chem.* **279,** 22483–22489
23. Holzbaur, E. L., and Vallee, R. B. (1994) *Annu. Rev. Cell Biol.* **10,** 339–372
24. Vallee, R. B., and Sheetz, M. P. (1996) *Science* **271,** 1539–1544
25. King, S. M., Barbarese, E., Dillman, J. F., III, Patel-King, R. S., Carson, J. H., and Pfister, K. K. (1996) *J. Biol. Chem.* **271,** 19358–19366
26. Jaffrey, S. R., and Snyder, S. H. (1996) *Science* **274,** 774–777
27. Puthalakath, H., Huang, D. C., O'Reilly, L. A., King, S. M., and Strasser, A. (1999) *Mol. Cell* **3,** 287–296
28. Puthalakath, H., Villunger, A., O'Reilly, L. A., Beaumont, J. G., Coultas, L., Cheney, R. E., Huang, D. C., and Strasser, A. (2001) *Science* **293,** 1829–1832
29. Schnorrer, F., Bohmann, K., and Nusslein-Volhard, C. (2000) *Nat. Cell Biol.* **2,** 185–190
30. Crepieux, P., Kwon, H., Leclerc, N., Spencer, W., Richard, S., Lin, R., and Hiscott, J. (1997) *Mol. Cell. Biol.* **17,** 7375–7385
31. Naisbitt, S., Valtschanoff, J., Allison, D. W., Sala, C., Kim, E., Craig, A. M., Weinberg, R. J., and Sheng, M. (2000) *J. Neurosci.* **20,** 4524–4534
32. Jacob, Y., Badrane, H., Ceccaldi, P. E., and Tordo, N. (2000) *J. Virol.* **74,** 10217–10222
33. Raux, H., Flamand, A., and Blondel, D. (2000) *J. Virol.* **74,** 10212–10216
34. Lo, K. W., Naisbitt, S., Fan, J. S., Sheng, M., and Zhang, M. (2001) *J. Biol. Chem.* **276,** 14059–14066
35. DiBella, L. M., Benashski, S. E., Tedford, H. W., Harrison, A., Patel-King, R. S., and King, S. M. (2001) *J. Biol. Chem.* **276,** 14366–14373
36. Fan, J. S., Zhang, Q., Tochio, H., Li, M., and Zhang, M. (2001) *J. Mol. Biol.* **306,** 97–108
37. Fan, J. S., Zhang, Q., Tochio, H., and Zhang, M. (2002) *J. Biomol. NMR* **23,** 103–114
38. Fan, J. S., Zhang, Q., Li, M., Tochio, H., Yamazaki, T., Shimizu, M., and Zhang, M. (1998) *J. Biol. Chem.* **273,** 33472–33481
39. Liang, J., Jaffrey, S. R., Guo, W., Snyder, S. H., and Clardy, J. (1999) *Nat. Struct. Biol.* **6,** 735–740
40. Rodriguez-Crespo, I., Yelamos, B., Roncal, F., Albar, J. P., Ortiz de Montellano, P. R., and Gavilanes, F. (2001) *FEBS Lett.* **503,** 135–141
41. Lindgren, M., Hallbrink, M., Prochiantz, A., and Langel, U. (2000) *Trends Pharmacol. Sci.* **21,** 99–103
42. Joliot, A., and Prochiantz, A. (2004) *Nat. Cell Biol.* **6,** 189–196
43. Passafaro, M., Sala, C., Niethammer, M., and Sheng, M. (1999) *Nat. Neurosci.* **2,** 1063–1069
44. Makokha, M., Hare, M., Li, M., Hays, T., and Barbar, E. (2002) *Biochemistry* **41,** 4302–4311
45. Ward, I. M., Minn, K., Jorda, K. G., and Chen, J. (2003) *J. Biol. Chem.* **278,** 19579–19582